Quantum Interference of Cavity Light Induced by a Single Atom in Double Well

Yijia Zhou,[1] Xinwei Li,[1] Weibin Li,[2] and Hao Zhang[1,*]

[1]*Graduate School of China Academy of Engineering Physics, Beijing 100193, China*
[2]*School of Physics and Astronomy and Centre for the Mathematics and Theoretical Physics of Quantum Non-Equilibrium Systems, The University of Nottingham, Nottingham, NG7 2RD, United Kingdom*

(Dated: June 13, 2023)

Interference in photons emitted from multiple atoms has been studied extensively. We show that a single atom can induce interference in its emitted light when tunnelling in a double-well potential coupled to an optical cavity. The phase in the cavity field interference can be modulated by the double-well spacing. By controlling the coherent tunnelling, blockade of single-photon excitations is found in the destructive interference regime, where super-Poissonian bunched light is generated. Furthermore, we show that the atomic flux of the coherent tunnelling motion generates chiral cavity fields. The direction of the chirality oscillates for many cycles before the decoherence of the atomic motion and the decay of the cavity photons. Our work opens new ways for manipulating photons with controllable quantum states of atoms for quantum information applications.

Understanding and controlling interference in light scattered from quantum emitters are crucial for achieving efficient light-matter coupling and building versatile quantum information devices. The quantum interference of radiation from two coherently driven atoms can produce rich spatial structures of nonclassical photon correlations [1–4]. Metasurfaces implemented with arrays of atoms can be employed to control light flow direction and manipulate photonic quantum states [5–8]. Engineering destructive interference between light and atomic subradiant excitation states allows tailored light storage and spectral narrowing [9–11] that has promising applications in quantum information processing and metrology. In addition to interference effects in free space, coupling atoms to an optical cavity that enhances the atom-light interaction enables exploration of collective radiation effects in the Tavis-Cummings model for multi-atom systems [12–14].

Previous efforts have focused on the interference of emissions from more than one emitter, including the Young's double-slit experiment with two ions [15], the measurement of collective frequency shift in resonant light scattered by a one-dimensional atomic array [16], observation of subradiance in dense atomic ensembles [17], demonstration of a two-dimensional atomic mirror [18], and measurements of the interference of cavity light from multiple atoms [19–22]. In these setups, the interference effect arises from the controllable mutual phase relations between spatially separated multiple atoms.

In this work, we ask a different question: whether *a single atom* can emit light with an interference pattern when prepared in a coherent superposition of different positions. The question is intuitively appealing, but there are two opposing arguments. One argument suggests that the optical fields emitted simultaneously by the single atom from different positions should interfere, while the other argument [23–25] states that the emitted light becomes entangled with the atomic position state and cannot interfere. To resolve this contradiction, we demonstrate that the coherent tunnelling between the atomic position states is the key to interference.

We present a new approach to manipulating and observing interference effects using only one atom. We consider an atom trapped in a double-well potential and coupled to an optical cavity as shown in Fig. 1(a). The coherent motion in the double-well produces quantum interference on the cavity field, resulting in a sinusoidal modulation of cavity emission as a function of the double-well spacing. The interference contrast can be continuously tuned by the atom's tunnelling amplitude. The atomic motion significantly influences the photon correlations of the cavity emission and can yield super-Poissonian bunched light near the destructive interference. Furthermore, we show that the coherent tunnelling motion of the single atom can be used to steer the light propagation direction, giving rise to persistent oscillations in the cavity directional emissions with the intensity difference proportional to the atomic flux in the double well. It also provides a non-destructive approach to monitoring atomic dynamics through cavity emission.

Our apparatus is shown in Fig. 1(a). We employ a ring-shaped optical cavity that supports two counterpropagating modes, denoted by the field operators $\hat{a}_{\rm CW}$ and $\hat{a}_{\rm CCW}$ for the clockwise (CW) and counter-clockwise (CCW) directions, respectively. The atom is driven by an external laser field that couples two internal states $|g\rangle$ and $|e\rangle$ with Rabi frequency Ω

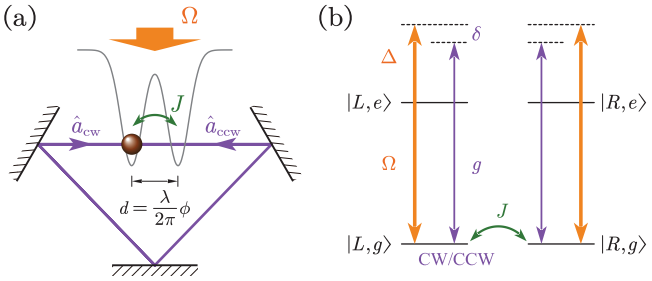

FIG. 1. (a) A single atom is confined in a double-well potential with spacing d and tunnelling amplitude J. The atom couples to an optical ring cavity with two counter-propagating modes, $\hat{a}_{\rm CW}$ and $\hat{a}_{\rm CCW}$, and is driven by an external light field with the Rabi frequency Ω. (b) The driving field is detuned from the atomic resonance by Δ, and the cavity modes by δ. The external states of the atom are denoted by $|L\rangle$ and $|R\rangle$.

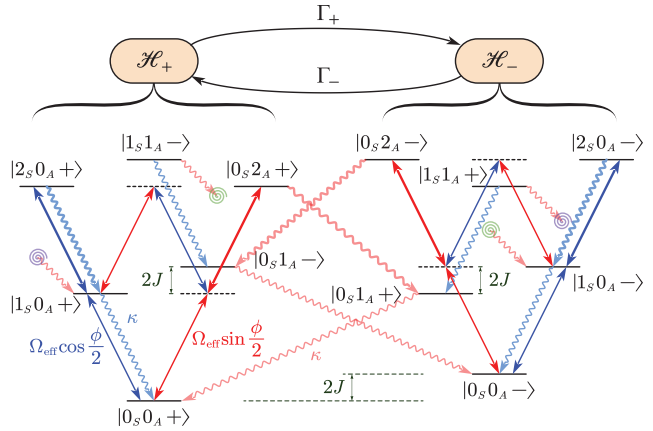

FIG. 2. The energy level diagram revealing the $\mathbb{Z}_2$ symmetry after transforming the external states from $\{|L\rangle, |R\rangle\}$ to $\{|+\rangle, |-\rangle\}$ basis and the cavity fields from $\{\hat{a}_{\rm CW}, \hat{a}_{\rm CCW}\}$ to $\{\hat{a}_S, \hat{a}_A\}$ modes. The energy splitting between $|+\rangle$ and $|-\rangle$ is $2J$. The excited state $|e\rangle$ is eliminated in the dispersive regime. The $\mathscr{H}_+$ subspace is spanned by the even-parity states, and $\mathscr{H}_-$ by the odd-parity states. The $\hat{a}_S$-mode is driven with the coupling strength $\Omega_{\rm eff}\cos\frac{\phi}{2}$ (blue arrows) and the $\hat{a}_A$-mode with $\Omega_{\rm eff}\sin\frac{\phi}{2}$ (red arrows). The cavity decays of the $\hat{a}_S$ and $\hat{a}_A$ modes are indicated by the blue and red wavy lines at the rate κ, and do not change the external states $|\pm\rangle$. However, the decay of the $\hat{a}_A$-mode photons leads to the population transfer between the subspaces $\mathscr{H}_+$ and $\mathscr{H}_-$ at the rates Γ_+ and Γ_-, which are proportional to the populations of $|0_S\,1_A-\rangle$ and $|0_S\,1_A+\rangle$ states, respectively. The purple and green spirals connect the relevant decay lines from the $|1_S\,1_A\pm\rangle$ states for illustration purposes.

as shown in Fig. 1(b). The detuning between the driving laser and the atomic resonance is $\Delta = \omega - \omega_a$, and the cavity detuning is $\delta = \omega - \omega_c$. The atomic tunnelling amplitude between the two wells is J. The atom-photon interaction depends on not only the atom-cavity coupling g, but also a phase factor e^{ikz_j} where z_j refers to the position of the atom along the cavity axis, and $k = \omega_c/c$ is the wave number of the cavity modes. The external states of the atom are denoted by $|L\rangle$ and $|R\rangle$ centred at $z_L = -d/2$ and $z_R = d/2$ with d being the double-well spacing. The spatial phase difference is given by $\phi = 2\pi d/\lambda$. The system is described by the Hamiltonian

$$\begin{aligned}\hat{H} = &-\delta\left(\hat{a}^\dagger_{\rm CW}\hat{a}_{\rm CW} + \hat{a}^\dagger_{\rm CCW}\hat{a}_{\rm CCW}\right) - \Delta\hat{\sigma}^+\hat{\sigma}^- + \frac{\Omega}{2}\hat{\sigma}^x \\ &+ g\left[\hat{\sigma}^+\sum_{j=L,R}\left(e^{i\phi_j}\hat{a}_{\rm CW} + e^{-i\phi_j}\hat{a}_{\rm CCW}\right)|j\rangle\langle j| + \text{H.c.}\right] \\ &- J\left(|L\rangle\langle R| + |R\rangle\langle L|\right),\end{aligned} \tag{1}$$

where $\hat{\sigma}^\pm$ and $\hat{\sigma}^x$ are the Pauli operators associated to $|g\rangle$ and $|e\rangle$, and $\phi_L = -\phi/2$, $\phi_R = \phi/2$. Due to the atomic spontaneous emission (rate γ) and the cavity decay (rate κ), the evolution of the total density matrix follows the Lindblad master equation, $\dot{\rho} = -i[\hat{H}, \rho] + \gamma\mathcal{D}[\hat{\sigma}^-]\rho + \kappa\mathcal{D}[\hat{a}_{\rm CW}]\rho + \kappa\mathcal{D}[\hat{a}_{\rm CCW}]\rho$, where $\mathcal{D}[\hat{L}]\rho = \hat{L}\rho\hat{L}^\dagger - \frac{1}{2}\{\hat{L}^\dagger\hat{L}, \rho\}$.

We notice that the Hamiltonian (1) has a $\mathbb{Z}_2$ symmetry, which can be better understood if we transform the atomic external state from the localized basis $\{|L\rangle, |R\rangle\}$ to the extended basis $\{|+\rangle = (|L\rangle + |R\rangle)/\sqrt{2}, |-\rangle = (|L\rangle - |R\rangle)/\sqrt{2}\}$, and the cavity fields from the $\hat{a}_{\rm CW}$, $\hat{a}_{\rm CCW}$ modes to $\hat{a}_S = (\hat{a}_{\rm CW} + \hat{a}_{\rm CCW})/\sqrt{2}$ and $\hat{a}_A = -i(\hat{a}_{\rm CW} - \hat{a}_{\rm CCW})/\sqrt{2}$. The total photon number $n_{\rm tot}$ is conserved in both representations, such that $n_{\rm tot} = \langle\hat{a}^\dagger_{\rm CW}\hat{a}_{\rm CW}\rangle + \langle\hat{a}^\dagger_{\rm CCW}\hat{a}_{\rm CCW}\rangle = \langle\hat{a}^\dagger_S\hat{a}_S\rangle + \langle\hat{a}^\dagger_A\hat{a}_A\rangle$. In this paper we focus on the dispersive regime where $g, \Omega \ll |\Delta|$ and the excited state $|e\rangle$ is adiabatically eliminated. The Hamiltonian of Eq. (1) is simplified to $H_{\rm eff} = H_S + H_A - J\hat{\sigma}^z_{\rm ext}$ with

$$H_S = -\delta\hat{a}^\dagger_S\hat{a}_S + \frac{\Omega_{\rm eff}}{2}\cos\frac{\phi}{2}\left(\hat{a}^\dagger_S + \hat{a}_S\right), \tag{2a}$$

$$H_A = -\delta\hat{a}^\dagger_A\hat{a}_A + \frac{\Omega_{\rm eff}}{2}\sin\frac{\phi}{2}\left(\hat{a}^\dagger_A + \hat{a}_A\right)\hat{\sigma}^x_{\rm ext}, \tag{2b}$$

where $\hat{\sigma}^x_{\rm ext} = |+\rangle\langle -| + |-\rangle\langle +|$, $\hat{\sigma}^z_{\rm ext} = |+\rangle\langle +| - |-\rangle\langle -|$, and $\Omega_{\rm eff} = \sqrt{2}g\Omega/\Delta$. The second term, H_A, is similar to the quantum Rabi model [26, 27]. The $\mathbb{Z}_2$ symmetry of $H_{\rm eff}$ is revealed by the parity operator $\hat{\Pi} = \exp(i\pi\hat{a}^\dagger_A\hat{a}_A)\hat{\sigma}^z_{\rm ext}$, which satisfies $[\hat{\Pi}, H_{\rm eff}] = 0$. Therefore, one can decompose the Hilbert space of $H_{\rm eff}$ into two subspaces according to the parity of the states, $\mathscr{H} = \mathscr{H}_+ \oplus \mathscr{H}_-$. Figure 2 shows the lowest 12 states categorized by the parity. For example, $|0_S, 0_A, +\rangle \in \mathscr{H}_+$ and $|0_S, 1_A, +\rangle \in \mathscr{H}_-$. While $H_{\rm eff}$ conserves the parity, the dissipation of $\hat{a}_A$-mode photon leads to the incoherent population transfer between $\mathscr{H}_+$ and $\mathscr{H}_-$ with the respective rates Γ_+ and Γ_- calculated below.

Using $H_{\rm eff}$ expressed in $\hat{a}_S$ and $\hat{a}_A$ basis [Eq. (2)], we calculate the total cavity photon number $n_{\rm tot}$ of the steady state (see Supplemental Materials, **SM**) as

$$n_{\rm tot} \simeq n_0\left(\cos^2\frac{\phi}{2} + \frac{1}{1 + 4J^2/(\delta^2 + \kappa^2/4)}\sin^2\frac{\phi}{2}\right), \tag{3}$$

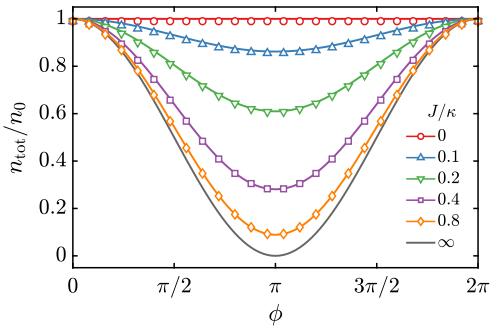

FIG. 3. Steady-state solutions to the cavity photon numbers with a single atom trapped in a double well driven on cavity resonance ($\delta = 0$). The cavity photon number, $n_{\rm tot}$, shows sinusoidal modulations as function of the double-well spacing denoted by $\phi = 2\pi d/\lambda$, normalized by the photon number n_0 of an atom trapped in a fixed position. The interference contrast increases with J/κ. The solid lines are the analytical results according to Eq. (3), and the points are the numerical solutions to the master equation. Other parameters are $(\gamma, \Delta, \kappa, g, \Omega) = (10, 200, 1, 0.5, 20)$, which are also applied to the rest of this work.

where $n_0 = 2 \times |g\Omega/(2\Delta)/(\delta + i\kappa/2)|^2$ is for an atom in a fixed position. The first term in Eq. (3) is the photon number of the $\hat{a}_S$-mode driven by $|0_S\, 0_A \pm\rangle \leftrightarrow |1_S\, 0_A \pm\rangle$ with the transition amplitude $\Omega_{\rm eff} \cos\frac{\phi}{2}$. The second term is the $\hat{a}_A$-mode driven by $|0_S\, 0_A \pm\rangle \leftrightarrow |0_S\, 1_A \mp\rangle$ with the transition amplitude $\Omega_{\rm eff} \sin\frac{\phi}{2}$ and the detuning $\pm 2J$.

Figure 3 shows the sinusoidal modulation of the cavity photon number $n_{\rm tot}$ as a function of the double-well spacing on the cavity resonance ($\delta = 0$). The $n_{\rm tot}$ interference contrast increases with J. When $J = 0$, the photon number is independent of ϕ ($n_{\rm tot} = n_0$), which agrees with the statement that the emitted light is entangled with the atomic position state so there is no interference effect [23–25]. In the limit $J \to \infty$, $n_{\rm tot}$ approaches to $n_0 \cos^2\frac{\phi}{2}$. This can be understood by the level diagram of Fig. 2. When $2J \gg \kappa/2$, the generation of the $\hat{a}_A$-mode photon is suppressed so the cavity field is dominated by the $\hat{a}_S$-mode, resulting in the interference pattern which is proportional to $\cos^2\frac{\phi}{2}$. From a complementary perspective, the light emitted by the atom at the position $|L\rangle$ is stored in the cavity over time $\sim 1/\kappa$. After the tunnelling time $\sim 1/J$, the atom emits light from the position $|R\rangle$. The two light fields can interfere if the tunnelling time is shorter than the cavity decay time ($1/J \ll 1/\kappa$).

The interference induced by the atomic tunnelling has a strong effect on the cavity photon statistics, which can be characterized by the second-order correlation function, $g^{(2)}(\tau) = \langle\hat{a}^\dagger\hat{a}^\dagger(\tau)\hat{a}(\tau)\hat{a}\rangle/\langle\hat{a}^\dagger\hat{a}\rangle^2$, with $\hat{a}$ being either $\hat{a}_{\rm CW}$ or $\hat{a}_{\rm CCW}$. We find that the analytical solution of $g^{(2)}(\tau)$ is the same for the two modes and reads (see **SM**)

$$g^{(2)}(\tau) = 1 + \left[1 + \left(1 + \frac{16J^2}{\kappa^2}\right)\cot^2\frac{\phi}{2}\right]^{-2} \times \left(\frac{16J^2}{\kappa^2}e^{-\kappa\tau} + \frac{8J}{\kappa}e^{-\kappa\tau/2}\sin 2J\tau\right). \tag{4}$$

The equal-time correlation $g^{(2)}(0)$ of the cavity emission is plotted in Fig. 4(a) as a function of ϕ, showing strong photon bunching near the destructive interference $\phi = \pi$. The peak value of $g^{(2)}(0)$ at $\phi = \pi$ increases quadratically with J/κ as shown in Fig. 4(b). At the destructive interference, the transition amplitudes of the $\hat{a}_S$-mode [the blue arrows in Fig. 2] are cancelled out as $\Omega_{\rm eff}\cos\frac{\phi}{2} = 0$, and only the $\hat{a}_A$-mode photons are generated as $\Omega_{\rm eff}\sin\frac{\phi}{2} = \Omega_{\rm eff}$. The level diagram is simplified to Fig. 4(c). When $2J \gg \kappa/2$, the one-photon excitations ($|0_A\rangle \to |1_A\rangle$) are far off-resonant and hence suppressed, while the simultaneous excitations of two photons ($|0_A\rangle \to |1_A\rangle \to |2_A\rangle$) are on-resonant, resulting in the photon-pair generation and huge photon bunching. The correlation $g^{(2)}(\tau)$ displays a temporal oscillation with the frequency $2J$ due to the cavity detuning from the $|0_A\pm\rangle \to |1_A\mp\rangle$ transitions as shown in Fig. 4(d).

Having studied the steady-state cavity interference and the photon correlations, we next examine the dynamical evolution of the cavity field before reaching the equilibrium. As the atom tunnels within the double well, directional emissions from the cavity can be generated, which oscillate at the tunnelling frequency J as depicted in Fig. 5(a). On the other hand, the backaction of the cavity field gives rise to the decoherence of the atomic tunnelling motion. If the tunnelling frequency J is large compared to the decoherence rate Γ (which will be derived later), the instantaneous cavity fields adiabatically follow the external state of the atom described by the reduced density matrix $\rho_{\rm ext}(t)$. To understand the physical picture, we examine the cavity fields in the mean-field approximation as $\alpha_\mu = \langle\hat{a}_\mu\rangle$, where $\hat{a}_\mu$ is either CW/CCW mode, or $\hat{a}_S/\hat{a}_A$-mode. In the adiabatic approximation (see **SM**)

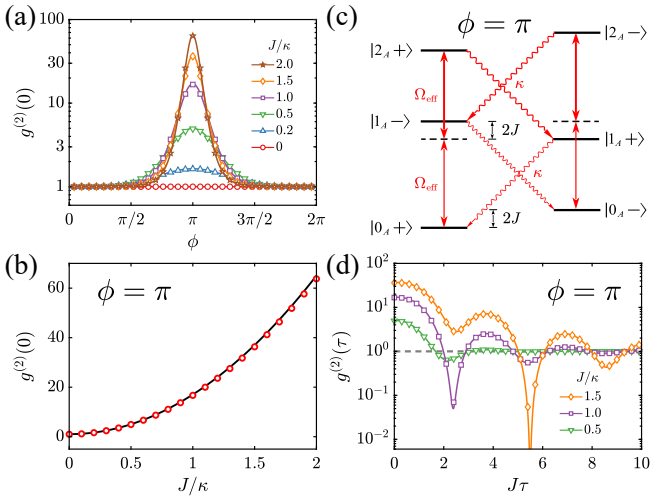

FIG. 4. Second-order correlation functions of the cavity emission at $\delta = 0$. (a) $g^{(2)}(0)$ as functions of ϕ for different values of J/κ indicating transitions from Poissonian near $\phi = 0$ to super-Poissonian near $\phi = \pi$. (b) The maximum values of $g^{(2)}(0)$ at $\phi = \pi$ compared with $g^{(2)}(0) = 1 + 16J^2/\kappa^2$ (solid black line). (c) The level diagram for $\phi = \pi$. The $\hat{a}_S$-mode photons in Fig. 2 are not excited due to the destructive interference hence not shown. The single-photon excitations of $\hat{a}_A$-mode are detuned by $\pm 2J$, which lead to the photon-pair generation and the photon bunching effect. (d) $g^{(2)}(\tau)$ at $\phi = \pi$ for different values of J/κ shows stronger oscillation amplitudes for larger tunnelling J. The oscillation frequency is $2J$ and the damping rate is given by κ. In (a,b,d), the points are the numerical simulation results and the solid lines are the analytical solutions Eq. (4).

$$\alpha_S = \frac{\Omega_{\rm eff}}{2}\frac{2}{\delta + i\kappa/2}\cos\frac{\phi}{2}, \tag{5a}$$

$$\alpha_A = \frac{\Omega_{\rm eff}}{2}\left(\frac{\rho^{+-}_{\rm ext}(t)}{\delta - 2J + i\kappa/2} + \frac{\rho^{-+}_{\rm ext}(t)}{\delta + 2J + i\kappa/2}\right)\sin\frac{\phi}{2}. \tag{5b}$$

At the early time $t \ll 1/\Gamma$ before the tunnelling motion decoheres, $\rho_{\rm ext}(t) \approx \frac{1}{2}(|+\rangle\langle+| + |-\rangle\langle-| + e^{2iJt}|+\rangle\langle-| + e^{-2iJt}|-\rangle\langle+|)$. Substituting $\rho_{\rm ext}(t)$ to Eq. (5), the evolution of $\alpha_{\rm CW/CCW}$ traces an ellipse in the phase space as shown in Fig. 5(b). When $\phi = \pi/2$ and $\delta = -J$, the amplitude $|\alpha_S|$ is comparable to $|\alpha_A|$ therefore $|\alpha_{\rm CW}|$ can be very different from $|\alpha_{\rm CCW}|$, resulting in directional emissions. When $\phi = \pi$, however, $\alpha_S = 0$ therefore the two fields have the same amplitudes but the opposite phases, $\alpha_{\rm CW} = -\alpha_{\rm CCW}$. We define the cavity chirality as

$$\Delta n/n_0 = (n_{\rm CW} - n_{\rm CCW})/n_0, \tag{6}$$

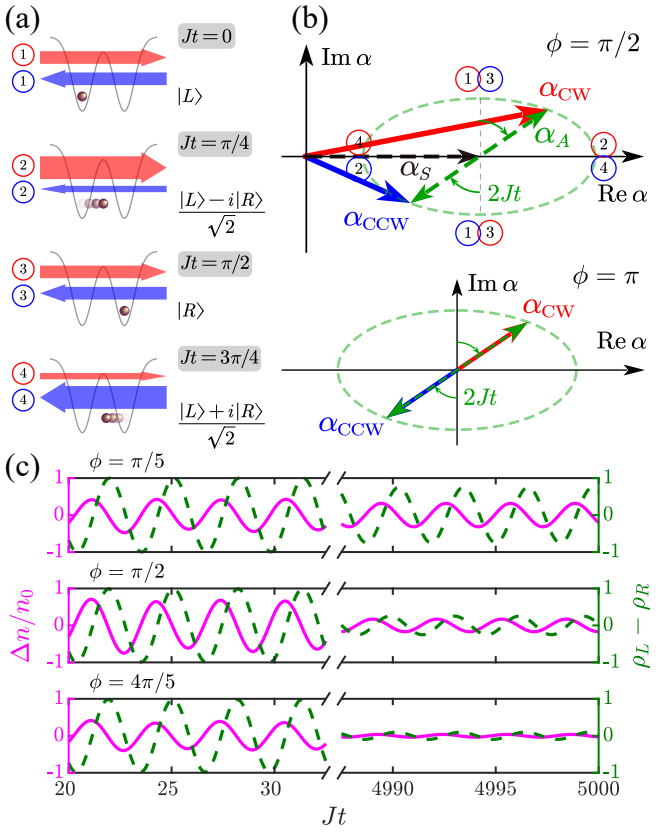

FIG. 5. Cavity chiral fields induced by the atomic motion. (a) The CW (red arrow) and CCW (blue arrow) modes are shown at different times of the atomic tunnelling motion for $\phi = \pi/2$. When the atom is in the superposition states $\frac{1}{\sqrt{2}}(|L\rangle \pm i|R\rangle)$ with the maximum tunnelling flux, the cavity fields have different intensities for the CW and CCW modes. (b) A sketch of the instantaneous cavity fields in the phase space for $\phi = \pi/2$ and $\phi = \pi$, where $\alpha = \langle\hat{a}\rangle$. The CW (red) and CCW (blue) modes are constructed by the $\hat{a}_S$- (black) and $\hat{a}_A$- (green) modes according to $\alpha_{\rm CW/CCW} = (\alpha_S \pm i\alpha_A)/\sqrt{2}$. The $\hat{a}_S$-mode is time-independent, while the $\hat{a}_A$-mode rotates at a frequency of $2J$. The green dashed ellipses represent the trajectories of $\alpha_{\rm CW}$ and $\alpha_{\rm CCW}$. When $\phi = \pi/2$, the magnitudes of $\alpha_{\rm CW}$ and $\alpha_{\rm CCW}$ oscillate at the frequency of $2J$. When $\phi = \pi$, $\alpha_S = 0$ therefore $|\alpha_{\rm CW}| = |\alpha_{\rm CCW}|$. The circled numbers correspond to the time steps in (a). (c) Numerical results of the dynamical evolution of $\Delta n/n_0 = (n_{\rm CW} - n_{\rm CCW})/n_0$ (solid magenta lines) and the atomic population difference between the left and right wells, $\rho_L - \rho_R$ (dashed green lines). Both the cavity field chirality and the atomic position oscillate at a frequency $2J$. Their phase difference is $\pi/2$. When the double-well spacing increases from $\phi = \pi/5$ to $\phi = 4\pi/5$, the decoherence rate Γ of the atomic tunnelling increases due to the backaction of the cavity light, resulting in the damping of the chiral cavity emissions. In the numerical simulations, the initial state of the atom is $|L\rangle$ with $-\delta = J = 5\kappa$.

where $n_{\rm CW/CCW} = \frac{1}{2}\langle(\hat{a}_S \pm i\hat{a}_A)^\dagger(\hat{a}_S \pm i\hat{a}_A)\rangle = \frac{1}{2}[n_S + n_A(t)] \pm {\rm Im}[\alpha_S\alpha_A^*(t)]$ (see **SM**). From Eq. (5)-(6), $\Delta n/n_0 \propto \sin\phi\, {\rm Im}\rho_{\rm ext}^{+-}$ when $\kappa \ll |\delta \pm 2J|$. Notice that ${\rm Im}\rho_{\rm ext}^{+-} = {\rm Im}\langle L|\rho_{\rm ext}|R\rangle$ indicates the atomic flux of the tunnelling motion from $|L\rangle$ to $|R\rangle$ in the double well. In Fig. 5(a), at $Jt = 0$ and $\pi/2$, the atomic flux is zero hence both the CW and CCW modes have the same photon numbers. At $Jt = \pi/4$ and $3\pi/4$, the atomic flux reaches the maximum value resulting in the cavity directional emission. Figure 5(c) shows the dynamical evolution of $\Delta n/n_0$ compared with the population difference in the double well, $\rho_L - \rho_R$, for different values of ϕ.

The backaction of the cavity field gives rise to the decoherence of the atomic tunnelling motion. To calculate the decoherence rate Γ, we obtain the master equation for the atomic external state $\dot{\rho}_{\rm ext} \approx -i[-J\hat{\sigma}_{\rm ext}^z,\ \rho_{\rm ext}] + (\Gamma_+\mathcal{D}[\hat{\sigma}_{\rm ext}^+] + \Gamma_-\mathcal{D}[\hat{\sigma}_{\rm ext}^-])\rho_{\rm ext}$ (see **SM**). The dissipator $\mathcal{D}[\hat{\sigma}_{\rm ext}^+]$ describes the incoherent population transfer from the subspace $\mathscr{H}_+$ to $\mathscr{H}_-$, and similarly $\mathcal{D}[\hat{\sigma}_{\rm ext}^-]$ the transfer from $\mathscr{H}_-$ to $\mathscr{H}_+$, as shown in Fig. 2. The respective rates are given by $\Gamma_\pm = \kappa\Omega_{\rm eff}^2/4[(\delta\mp 2J)^2+\kappa^2/4]^{-1}\sin^2\frac{\phi}{2}$, which correspond to the cavity photon generation as $\kappa n_A(t) = \Gamma_+\rho_{\rm ext}^{++}(t) + \Gamma_-\rho_{\rm ext}^{--}(t)$. With the initial state being $\rho_{\rm ext}(0) = |L\rangle\langle L|$, the reduced density matrix of the external state evolves as $\rho_{\rm ext}^{-+} = e^{-\Gamma t/2}e^{i2Jt}$, where $\Gamma = \Gamma_+ + \Gamma_-$ is modulated by $\sin^2\frac{\phi}{2}$. As shown in Fig. 5(c), the decoherence is faster for $\phi \approx \pi$ than $\phi \approx 0$. In the dispersive regime, Γ is several orders smaller than κ and J, which allows for many cycles of the oscillation before the decoherence of the atomic motion and the leakage of the cavity photons.

In summary, we have demonstrated that a single atom can induce interference effects in light by studying a minimal model comprising one atom tunnelling in a double-well potential coupled to an optical ring cavity. The atom's coherent tunnelling gives rise to cavity field interference, photon-pair generation, and directional emission. This work can be readily extended in various directions. First, we can expand our analysis beyond the scenario where the chiral cavity fields adiabatically follow the atomic tunnelling motion. By exploring the regime where the light fields substantially modify the tunnelling frequency, we can investigate the entanglement between the atomic motional state and the chiral emission. Second, both the atomic motional states in the double well and the cavity chiral photons can be utilized to encode qubits. Their entanglement allows for new gate operation schemes and our apparatus may serve as quantum nodes in cavity-based quantum networks. Furthermore, our current minimal model of a single atom in the double well can be extended to multiple atoms tunnelling in a lattice. Cavity emission can provide non-destructive measurements of atomic collective motion, such as Bloch oscillation, superfluid-Mott insulator transition, and self-organization.

The authors thank Chang-Pu Sun and Markus Müller for insightful discussions. This work was supported by the National Key Research and Development Program of China (Grant No. 2022YFA1405300), National Natural Science Foundation of China (Grant No. 12088101). WL acknowledges support of an International Research Collaboration Fund of the University of Nottingham.

* hzhang@gscaep.ac.cn

[1] W. Vogel and D. G. Welsch, Squeezing Pattern in Resonance

Fluorescence from a Regular N-Atom System, Phys. Rev. Lett. **54**, 1802 (1985).
[2] C. Skornia, J. von Zanthier, G. S. Agarwal, E. Werner, and H. Walther, Nonclassical interference effects in the radiation from coherently driven uncorrelated atoms, Phys. Rev. A **64**, 063801 (2001).
[3] R. Wiegner, J. von Zanthier, and G. S. Agarwal, Quantum-interference-initiated superradiant and subradiant emission from entangled atoms, Phys. Rev. A **84**, 023805 (2011).
[4] S. Wolf, S. Richter, J. von Zanthier, and F. Schmidt-Kaler, Light of Two Atoms in Free Space: Bunching or Antibunching?, Phys. Rev. Lett. **124**, 063603 (2020).
[5] P.-O. Guimond, A. Grankin, D. V. Vasilyev, B. Vermersch, and P. Zoller, Subradiant Bell States in Distant Atomic Arrays, Phys. Rev. Lett. **122**, 093601 (2019).
[6] R. Bekenstein, I. Pikovski, H. Pichler, E. Shahmoon, S. F. Yelin, and M. D. Lukin, Quantum metasurfaces with atom arrays, Nat. Phys. **16**, 676 (2020).
[7] K. E. Ballantine and J. Ruostekoski, Quantum Single-Photon Control, Storage, and Entanglement Generation with Planar Atomic Arrays, PRX Quantum **2**, 040362 (2021).
[8] D. Fernández-Fernández and A. González-Tudela, Tunable Directional Emission and Collective Dissipation with Quantum Metasurfaces, Phys. Rev. Lett. **128**, 113601 (2022).
[9] G. Facchinetti, S. D. Jenkins, and J. Ruostekoski, Storing Light with Subradiant Correlations in Arrays of Atoms, Phys. Rev. Lett. **117**, 243601 (2016).
[10] A. Asenjo-Garcia, M. Moreno-Cardoner, A. Albrecht, H. J. Kimble, and D. E. Chang, Exponential Improvement in Photon Storage Fidelities Using Subradiance and "Selective Radiance" in Atomic Arrays, Phys. Rev. X **7**, 031024 (2017).
[11] S. J. Masson, I. Ferrier-Barbut, L. A. Orozco, A. Browaeys, and A. Asenjo-Garcia, Many-Body Signatures of Collective Decay in Atomic Chains, Phys. Rev. Lett. **125**, 263601 (2020).
[12] M. Tavis and F. W. Cummings, Exact Solution for an N-Molecule—Radiation-Field Hamiltonian, Phys. Rev. **170**, 379 (1968).
[13] P. Forn-Díaz, L. Lamata, E. Rico, J. Kono, and E. Solano, Ultrastrong coupling regimes of light-matter interaction, Rev. Mod. Phys. **91**, 025005 (2019).
[14] A. Frisk Kockum, A. Miranowicz, S. De Liberato, S. Savasta, and F. Nori, Ultrastrong coupling between light and matter, Nat. Rev. Phys. **1**, 19 (2019).
[15] U. Eichmann, J. C. Bergquist, J. J. Bollinger, J. M. Gilligan, W. M. Itano, D. J. Wineland, and M. G. Raizen, Young's interference experiment with light scattered from two atoms, Phys. Rev. Lett. **70**, 2359 (1993).
[16] A. Glicenstein, G. Ferioli, N. Šibalić, L. Brossard, I. Ferrier-Barbut, and A. Browaeys, Collective Shift in Resonant Light Scattering by a One-Dimensional Atomic Chain, Phys. Rev. Lett. **124**, 253602 (2020).
[17] G. Ferioli, A. Glicenstein, L. Henriet, I. Ferrier-Barbut, and A. Browaeys, Storage and Release of Subradiant Excitations in a Dense Atomic Cloud, Phys. Rev. X **11**, 021031 (2021).
[18] J. Rui, D. Wei, A. Rubio-Abadal, S. Hollerith, J. Zeiher, D. M. Stamper-Kurn, C. Gross, and I. Bloch, A subradiant optical mirror formed by a single structured atomic layer, Nature **583**, 369 (2020).
[19] R. Reimann, W. Alt, T. Kampschulte, T. Macha, L. Ratschbacher, N. Thau, S. Yoon, and D. Meschede, Cavity-Modified Collective Rayleigh Scattering of Two Atoms, Phys. Rev. Lett. **114**, 023601 (2015).
[20] A. Neuzner, M. Körber, O. Morin, S. Ritter, and G. Rempe, Interference and dynamics of light from a distance-controlled atom pair in an optical cavity, Nat. Photonics **10**, 303 (2016).
[21] M. A. Norcia, M. N. Winchester, J. R. K. Cline, and J. K. Thompson, Superradiance on the millihertz linewidth strontium clock transition, Sci. Adv. **2**, e1601231 (2016).
[22] J. Kim, D. Yang, S.-h. Oh, and K. An, Coherent single-atom superradiance, Science **359**, 662 (2018).
[23] C. Cohen-Tannoudji, F. Bardou, and A. Aspect, Review on fundamental processes in laser cooling, in *Laser Spectrosc. X*, edited by M. Ducloy, E. Giacobino, and G. Camy (World Scientific, Font-Romeu, France, 1992) pp. 3–14.
[24] D. Braun and J. Martin, Spontaneous emission from a two-level atom tunneling in a double-well potential, Phys. Rev. A **77**, 032102 (2008).
[25] F. Damanet, D. Braun, and J. Martin, Cooperative spontaneous emission from indistinguishable atoms in arbitrary motional quantum states, Phys. Rev. A **94**, 033838 (2016).
[26] D. Braak, Integrability of the Rabi Model, Phys. Rev. Lett. **107**, 100401 (2011).
[27] Q.-H. Chen, C. Wang, S. He, T. Liu, and K.-L. Wang, Exact solvability of the quantum Rabi model using Bogoliubov operators, Phys. Rev. A **86**, 023822 (2012).

Supplemental Materials for "Quantum Interference of Cavity Light Induced by a Single Atom in Double Well"

Yijia Zhou,[1] Xinwei Li,[1] Weibin Li,[2] and Hao Zhang[1]

[1]*Graduate School of China Academy of Engineering Physics, Beijing 100193, China*

[2]*School of Physics and Astronomy and Centre for the Mathematics and Theoretical Physics of Quantum Non-Equilibrium Systems, The University of Nottingham, Nottingham, NG7 2RD, United Kingdom*

(Dated: June 12, 2023)

I. Analytical solutions of the photon fields in the dispersive regime

The original Hamiltonian of the cavity QED system with a single atom coupled with two propagating cavity modes and trapped in a double-well potential under rotating frame is

$$\begin{aligned} H = &-\delta\left(\hat{a}_{\mathrm{CW}}^{\dagger}\hat{a}_{\mathrm{CW}} + \hat{a}_{\mathrm{CCW}}^{\dagger}\hat{a}_{\mathrm{CCW}}\right) - \Delta\,|e\rangle\langle e| + \frac{\Omega}{2}\hat{\sigma}^{x} - J\left(|L\rangle\langle R| + |R\rangle\langle L|\right) \\ &+ g\left\{\left[\left(e^{i\mathbf{k}_{\mathrm{CW}}\cdot\mathbf{r}_{L}}\hat{a}_{\mathrm{CW}} + e^{i\mathbf{k}_{\mathrm{CW}}\cdot\mathbf{r}_{R}}\hat{a}_{\mathrm{CCW}}\right)|L\rangle\langle L| + \left(e^{i\mathbf{k}_{\mathrm{CCW}}\cdot\mathbf{r}_{L}}\hat{a}_{\mathrm{CW}} + e^{i\mathbf{k}_{\mathrm{CCW}}\cdot\mathbf{r}_{R}}\hat{a}_{\mathrm{CCW}}\right)|R\rangle\langle R|\right]\hat{\sigma}^{+} + \mathrm{H.c.}\right\}, \end{aligned} \tag{1}$$

where the external state $|L\rangle$ and $|R\rangle$ denotes the atmoic position which is along the z-axis, such that $\mathbf{r}_{L/R} = (0, 0, z_{L/R})$. The wave vector of the CW and CCW modes are $\mathbf{k}_{\mathrm{CW}} = (0, 0, k)$ and $\mathbf{k}_{\mathrm{CCW}} = (0, 0, -k)$ near the double well, respectively. Due to translational symmetry, it is convenient to define $kz_L = -\phi/2$ and $kz_R = \phi/2$, and the double-well spacing is denoted by $d = \phi/(2\pi)\lambda$, with λ being the wavelength of the cavity fields. The atomic decay and photon loss can be described by Lindblad master equation,

$$\frac{\partial}{\partial t}\rho = -i[H, \rho] + \gamma\mathcal{D}[\hat{\sigma}^{-}]\rho + \kappa\mathcal{D}[\hat{a}_{\mathrm{CW}}]\rho + \kappa\mathcal{D}[\hat{a}_{\mathrm{CCW}}]\rho, \tag{2}$$

where $\mathcal{D}[\hat{L}]\rho = \hat{L}\rho\hat{L}^{\dagger} - \frac{1}{2}\{\hat{L}^{\dagger}\hat{L}, \rho\}$. Our numerical simulations are based on the time integration of Eq. (2).

The dispersive regime is valid when the atomic detuning is far bigger than the atomic and photonic dissipation rates and the atom-light interaction strength, $\Delta \gg \gamma, \kappa, g$, such that the atomic internal state can reach equilibrium faster than other time scales. In this situation, the original Hamiltonian can be simplified by adiabatic elimination. First of all, it is convenient to use the superposed photon modes as described in the main text,

$$\begin{aligned} \hat{a}_{S} &= \frac{1}{\sqrt{2}}\left(\hat{a}_{\mathrm{CW}} + \hat{a}_{\mathrm{CCW}}\right), \\ \hat{a}_{A} &= \frac{-i}{\sqrt{2}}\left(\hat{a}_{\mathrm{CW}} - \hat{a}_{\mathrm{CCW}}\right), \end{aligned} \tag{3}$$

which automatically gaurantees that $\mathcal{D}[\hat{a}_{\mathrm{CW}}]+\mathcal{D}[\hat{a}_{\mathrm{CCW}}] = \mathcal{D}[\hat{a}_{S}]+\mathcal{D}[\hat{a}_{A}]$. The atomic external states should also be symmetrized as

$$\begin{aligned} |+\rangle &= \frac{1}{\sqrt{2}}\left(|L\rangle + |R\rangle\right), \\ |-\rangle &= \frac{1}{\sqrt{2}}\left(|L\rangle - |R\rangle\right). \end{aligned} \tag{4}$$

Then, the tunnelling term reads $H_{\mathrm{ext}} = -J\hat{\sigma}_{\mathrm{ext}}^{z}$, with the Pauli matrices for the external states being $\hat{\sigma}_{\mathrm{ext}}^{z} = |+\rangle\langle+| - |-\rangle\langle-|$ and $\hat{\sigma}_{\mathrm{ext}}^{x} = |+\rangle\langle-| + |-\rangle\langle+|$. Then, we rewrite the original master equation [Eq. (2)] as

$$\frac{\partial}{\partial t}\rho = -i\left[\left(H_{g,\mathrm{nH}} + H_{e,\mathrm{nH}}\right)\rho - \rho\left(H_{g,\mathrm{nH}} + H_{e,\mathrm{nH}}\right)^{\dagger}\right] - i\left[V + V^{\dagger}, \rho\right] + \gamma\hat{\sigma}^{-}\rho\hat{\sigma}^{+} + \kappa\hat{a}_{\mathrm{CW}}\rho\hat{a}_{\mathrm{CW}}^{\dagger} + \kappa\hat{a}_{\mathrm{CCW}}\rho\hat{a}_{\mathrm{CCW}}^{\dagger}, \tag{5}$$

where

$$\begin{aligned} H_{g,\mathrm{nH}} &= -\left(\delta + i\frac{\kappa}{2}\right)\left(\hat{a}_S^\dagger \hat{a}_S + \hat{a}_A^\dagger \hat{a}_A\right) - J\hat{\sigma}_{\mathrm{ext}}^z, \\ H_{e,\mathrm{nH}} &= -\left(\Delta + i\frac{\gamma}{2}\right)|e\rangle\langle e|, \\ V &= \left(g\hat{A}^\dagger + \frac{\Omega}{2}\right)\hat{\sigma}^-, \\ \hat{A} &= \left(e^{-i\phi/2}\hat{a}_{\mathrm{CW}} + e^{i\phi/2}\hat{a}_{\mathrm{CCW}}\right)|L\rangle\langle L| + \left(e^{i\phi/2}\hat{a}_{\mathrm{CW}} + e^{-i\phi/2}\hat{a}_{\mathrm{CCW}}\right)|R\rangle\langle R| \\ &= \sqrt{2}\left(\cos\frac{\phi}{2}\hat{a}_S + \sin\frac{\phi}{2}\hat{a}_A\hat{\sigma}_{\mathrm{ext}}^x\right). \end{aligned} \tag{6}$$

Finally, the excited state $|e\rangle$ can be eliminated resulting in the effective Hamiltonian and dissipator [1]

$$\begin{aligned} H_{\mathrm{eff,nH}} &= H_{g,\mathrm{nH}} - V\frac{1}{H_{e,\mathrm{nH}}}V^\dagger \\ &= H_{g,\mathrm{nH}} + \frac{1}{\Delta + i\gamma/2}\left[g^2\hat{A}^\dagger\hat{A} + \frac{g\Omega}{2}\left(\hat{A}^\dagger + \hat{A}\right) + \frac{\Omega^2}{4}\right], \\ \hat{L}_{\mathrm{eff}} &= \hat{\sigma}^-\frac{1}{H_{e,\mathrm{nH}}}V^\dagger = -\frac{g\hat{A} + \frac{\Omega}{2}}{\Delta + i\gamma/2}|g\rangle\langle g|. \end{aligned} \tag{7}$$

In the dispersive regime, $\langle\hat{A}^\dagger\hat{A}\rangle \ll \mathrm{Re}\langle\hat{A}\rangle$, which allows us to neglect the $\hat{A}^\dagger\hat{A}$ term in Eq. (7) and keep the linear terms only. The decay rate of the dissipator $\hat{L}_{\mathrm{eff}}$ is in the order of $\gamma(g^2\langle\hat{A}^\dagger\hat{A}\rangle + \Omega^2)/\Delta^2$, which, in the dispersive regime, is much smaller than the decay rate of the cavity photon, κ, so $\hat{L}_{\mathrm{eff}}$ can be neglected as well as the corresponding imaginary part of $H_{\mathrm{eff,nH}}$. Therefore, the original master equation [Eq. (2)] can be simplified as

$$\frac{\partial}{\partial t}\rho = -i[H_{\mathrm{eff}}, \rho] + \kappa\mathcal{D}[\hat{a}_S]\rho + \kappa\mathcal{D}[\hat{a}_A]\rho, \tag{8}$$

with

$$\begin{aligned} H_{\mathrm{eff}} &= H_S + H_A - J\hat{\sigma}_{\mathrm{ext}}^z, \\ H_S &= -\delta\hat{a}_S^\dagger\hat{a}_S + \frac{\Omega_{\mathrm{eff}}}{2}\cos\frac{\phi}{2}\left(\hat{a}_S^\dagger + \hat{a}_S\right), \\ H_A &= -\delta\hat{a}_A^\dagger\hat{a}_A + \frac{\Omega_{\mathrm{eff}}}{2}\sin\frac{\phi}{2}\left(\hat{a}_A^\dagger + \hat{a}_A\right)\hat{\sigma}_{\mathrm{ext}}^x. \end{aligned} \tag{9}$$

The effective Rabi frequency $\Omega_{\mathrm{eff}} = \sqrt{2}g\Omega\Delta/(\Delta^2 + \gamma^2/4) \approx \sqrt{2}g\Omega/\Delta$.

Here we note that if one omits the external state, Eq. (8)-(9) can be used to describe the single atom trapped in a single-well. Considering the Heisenberg equations of the photon field operators, $i\partial_t\hat{a}_S = -(\delta + i\kappa/2)\hat{a}_S + \frac{\Omega_{\mathrm{eff}}}{2}\cos\frac{\phi}{2}$ and $i\partial_t\hat{a}_A = -(\delta + i\kappa/2)\hat{a}_A + \frac{\Omega_{\mathrm{eff}}}{2}\sin\frac{\phi}{2}$, one can obtain the photon numbers of the steady state

$$n_0 = |\alpha_S|^2 + |\alpha_A|^2 = \left|\frac{\Omega_{\mathrm{eff}}}{2}\frac{1}{\delta + i\kappa/2}\right|^2, \tag{10}$$

with $\alpha_S = \langle\hat{a}_S\rangle = \frac{\Omega_{\mathrm{eff}}}{2}\frac{1}{\delta+i\kappa/2}\cos\frac{\phi}{2}$ and $\alpha_A = \langle\hat{a}_A\rangle = \frac{\Omega_{\mathrm{eff}}}{2}\frac{1}{\delta+i\kappa/2}\sin\frac{\phi}{2}$.

However, if the atomic motion is included, the $\hat{a}_A$-mode cavity field is different from the ordinary bosonic field, because creating an A-mode photon flips the external state. Specifically, the Heisenberg equation of $\hat{a}_A$ becomes $i\partial_t\hat{a}_A = -(\delta + i\kappa/2)\hat{a}_A + \frac{\Omega_{\mathrm{eff}}}{2}\sin\frac{\phi}{2}\hat{\sigma}_{\mathrm{ext}}^x$. Now, $\hat{\sigma}_{\mathrm{ext}}^x$ oscillates at the frequency $\sim 2J$, which precludes the quasistatic condition by letting $\partial_t\hat{a}_A = 0$. To resolve this problem, we notice that the transitions of $|n_A, +\rangle \to |(n-1)_A, -\rangle$ or $|n_A, -\rangle \to |(n-1)_A, +\rangle$ can be triggered by $\hat{a}_A\hat{\sigma}_{\mathrm{ext}}^-$ and $\hat{a}_A\hat{\sigma}_{\mathrm{ext}}^+$, respectively. Therefore, we consider the Heisenberg equations of $\hat{a}_S$, $\hat{a}_A\hat{\sigma}_{\mathrm{ext}}^+$ and $\hat{a}_A\hat{\sigma}_{\mathrm{ext}}^-$ that read

$$\begin{aligned} i\frac{\partial}{\partial t}\hat{a}_S &= -\left(\delta + i\frac{\kappa}{2}\right)\hat{a}_S + \frac{\Omega_{\mathrm{eff}}}{2}\cos\frac{\phi}{2}, \\ i\frac{\partial}{\partial t}\hat{a}_A\hat{\sigma}_{\mathrm{ext}}^+ &= -\left(\delta + 2J + i\frac{\kappa}{2}\right)\hat{a}_A\hat{\sigma}_{\mathrm{ext}}^+ + \frac{\Omega_{\mathrm{eff}}}{2}\sin\frac{\phi}{2}\left[\hat{\sigma}_{\mathrm{ext}}^+\hat{\sigma}_{\mathrm{ext}}^- - \left(\hat{a}_A + \hat{a}_A^\dagger\right)\hat{a}_A\hat{\sigma}_{\mathrm{ext}}^z\right], \\ i\frac{\partial}{\partial t}\hat{a}_A\hat{\sigma}_{\mathrm{ext}}^- &= -\left(\delta - 2J + i\frac{\kappa}{2}\right)\hat{a}_A\hat{\sigma}_{\mathrm{ext}}^- + \frac{\Omega_{\mathrm{eff}}}{2}\sin\frac{\phi}{2}\left[\hat{\sigma}_{\mathrm{ext}}^-\hat{\sigma}_{\mathrm{ext}}^+ + \left(\hat{a}_A + \hat{a}_A^\dagger\right)\hat{a}_A\hat{\sigma}_{\mathrm{ext}}^z\right]. \end{aligned} \tag{11}$$

Then, one can let the left-hand-side equal to 0 for the quasistatic solutions for the given external state, because the evolution rate of $\hat{\sigma}^z_{\rm ext}$, as well as $\hat{\sigma}^\pm_{\rm ext}\hat{\sigma}^\mp_{\rm ext}$, is in the order of $\Gamma \ll J$ (see below). In the dispersive regime, the photon number is small, and we can further neglect the normal order terms with multiple $\hat{a}_A$ terms on the right-hand-side. Therefore, the adiabatic elimination can be carried out by taking the quantum expectation values of Eq. (11) that yields

$$\begin{aligned}
\langle \hat{a}_S \rangle &\approx \frac{\Omega_{\rm eff}/2}{\delta + i\kappa/2} \cos\frac{\phi}{2}, \\
\langle \hat{a}_A \hat{\sigma}^+_{\rm ext} \rangle &\approx \frac{\Omega_{\rm eff}/2}{\delta + 2J + i\kappa/2} \sin\frac{\phi}{2} \langle \hat{\sigma}^+_{\rm ext}\hat{\sigma}^-_{\rm ext} \rangle, \\
\langle \hat{a}_A \hat{\sigma}^-_{\rm ext} \rangle &\approx \frac{\Omega_{\rm eff}/2}{\delta - 2J + i\kappa/2} \sin\frac{\phi}{2} \langle \hat{\sigma}^-_{\rm ext}\hat{\sigma}^+_{\rm ext} \rangle .
\end{aligned} \tag{12}$$

We introduce the reduced density matrix of the external state, $\rho_{\rm ext} = {\rm Tr}_{\rm ph}[\rho]$, and $\rho^{++}_{\rm ext} = \langle \hat{\sigma}^-_{\rm ext}\hat{\sigma}^+_{\rm ext} \rangle$, $\rho^{--}_{\rm ext} = \langle \hat{\sigma}^+_{\rm ext}\hat{\sigma}^-_{\rm ext} \rangle$, $\rho^{+-}_{\rm ext} = \langle \hat{\sigma}^+_{\rm ext} \rangle$, $\rho^{-+}_{\rm ext} = \langle \hat{\sigma}^-_{\rm ext} \rangle$. Based on Eq. (12), one can use the substitution

$$\begin{aligned}
\hat{a}_S &\to \frac{\Omega_{\rm eff}/2}{\delta + i\kappa/2} \cos\frac{\phi}{2}, \\
\hat{a}_A &\to \frac{\Omega_{\rm eff}/2}{\delta + 2J + i\kappa/2} \sin\frac{\phi}{2} \overleftarrow{\hat{\sigma}^-_{\rm ext}} + \frac{\Omega_{\rm eff}/2}{\delta - 2J + i\kappa/2} \sin\frac{\phi}{2} \overleftarrow{\hat{\sigma}^+_{\rm ext}},
\end{aligned} \tag{13}$$

where $\overleftarrow{\sigma}$ refers to that the operator is applied on the right side of the other operators. With this substitution and using the identity $\hat{\sigma}^-_{\rm ext}\hat{\sigma}^+_{\rm ext} + \hat{\sigma}^+_{\rm ext}\hat{\sigma}^-_{\rm ext} = \mathbb{I}$, the complex light fields of the $\hat{a}_S$- and $\hat{a}_A$-modes are given by

$$\begin{aligned}
\alpha_S &= \frac{\Omega_{\rm eff}/2}{\delta + i\kappa/2} \cos\frac{\phi}{2}, \\
\alpha_A &= \langle \hat{a}_A \left(\hat{\sigma}^-_{\rm ext}\hat{\sigma}^+_{\rm ext} + \hat{\sigma}^+_{\rm ext}\hat{\sigma}^-_{\rm ext} \right) \rangle \\
&= \frac{\Omega_{\rm eff}/2}{\delta + 2J + i\kappa/2} \sin\frac{\phi}{2} \langle \hat{\sigma}^-_{\rm ext} \rangle + \frac{\Omega_{\rm eff}/2}{\delta - 2J + i\kappa/2} \sin\frac{\phi}{2} \langle \hat{\sigma}^+_{\rm ext} \rangle .
\end{aligned} \tag{14}$$

The photon numbers yield

$$\begin{aligned}
n_S &= \left| \frac{\Omega_{\rm eff}/2}{\delta + i\kappa/2} \cos\frac{\phi}{2} \right|^2 , \\
n_A &= \left\langle \hat{a}^\dagger_A \left(\hat{\sigma}^+_{\rm ext}\hat{\sigma}^-_{\rm ext} + \hat{\sigma}^-_{\rm ext}\hat{\sigma}^+_{\rm ext} \right) \hat{a}_A \right\rangle \\
&= \left| \frac{\Omega_{\rm eff}/2}{\delta + 2J + i\kappa/2} \sin\frac{\phi}{2} \right|^2 \langle \hat{\sigma}^+_{\rm ext}\hat{\sigma}^-_{\rm ext} \rangle + \left| \frac{\Omega_{\rm eff}/2}{\delta - 2J + i\kappa/2} \sin\frac{\phi}{2} \right|^2 \langle \hat{\sigma}^-_{\rm ext}\hat{\sigma}^+_{\rm ext} \rangle .
\end{aligned} \tag{15}$$

Therefore, we obtain the photon numbers of the CW and CCW modes,

$$\begin{aligned}
n_{\rm CW/CCW} &= \frac{1}{2} \left\langle \left(\hat{a}_S \pm i\hat{a}_A \right)^\dagger \left(\hat{a}_S \pm i\hat{a}_A \right) \right\rangle = \frac{1}{2} \left[n_S + n_A \pm i \left(\alpha^*_S \alpha_A - \alpha^*_A \alpha_S \right) \right] \\
&= \frac{n_0}{2} \left[\cos^2\frac{\phi}{2} + \sin^2\frac{\phi}{2} \left(\left| \frac{\delta + i\kappa/2}{\delta + 2J + i\kappa/2} \right|^2 \rho^{--}_{\rm ext} + \left| \frac{\delta + i\kappa/2}{\delta - 2J + i\kappa/2} \right|^2 \rho^{++}_{\rm ext} \right) \pm {\rm Im} \frac{4J\delta \sin\phi}{(\delta + 2J + i\kappa/2)(\delta - 2J - i\kappa/2)} \rho^{-+}_{\rm ext} \right] .
\end{aligned} \tag{16}$$

II. Dynamics of the atomic motion influenced by the cavity photons

In order to obtain the effective master equation of the atomic motion, we eliminate the photonic excited states with the adiabatic approximation. The $\hat{a}_S$-mode photons can be directly dropped out. In the dispersive regime, the $\hat{a}_A$-mode photon number can be truncated at $n_A \leqslant 1$, which results in 4 states, $|n_A, m\rangle \in \{|0_A, +\rangle, |0_A, -\rangle, |1_A, +\rangle, |1_A, -\rangle\}$. The non-Hermitian Hamiltonian reads

$$H_{\rm nH} = \begin{pmatrix}
-J & & & \frac{\Omega_{\rm eff}}{2}\sin\frac{\phi}{2} \\
 & J & \frac{\Omega_{\rm eff}}{2}\sin\frac{\phi}{2} & \\
 & \frac{\Omega_{\rm eff}}{2}\sin\frac{\phi}{2} & -J - \delta - i\frac{\kappa}{2} & \\
\frac{\Omega_{\rm eff}}{2}\sin\frac{\phi}{2} & & & J - \delta - i\frac{\kappa}{2}
\end{pmatrix} . \tag{17}$$

The quantum jump operators include $\hat{L}_- = |0_A, +\rangle\langle 1_A, -|$ and $\hat{L}_+ = |0_A, -\rangle\langle 1_A, +|$ with rates both equal to κ. To perform the adiabatic elimination, we introduce the projection operator $\mathcal{P} = |0_A, +\rangle\langle 0_A, +| + |0_A, -\rangle\langle 0_A, -|$ and $\mathcal{Q} = |1_A, +\rangle\langle 1_A, +| +$

$|1_A,-\rangle\langle 1_A,-|$. Noticing that $\mathcal{P}H_{\rm nH}\mathcal{P}$ is already diagonalized, we define the interaction operators acting on each of the vacuum states, $V_l = |l\rangle\langle l|\, H_{\rm nH}\mathcal{Q}$, with $|l\rangle \in \{|0_A,+\rangle, |0_A,-\rangle\}$. Then we obtain the effective non-Hermitian Hamiltonian and the dissipators that read [1]

$$\begin{aligned} H_{\rm ext,nH} &= \mathcal{P}H_{\rm nH}\mathcal{P} - V\sum_l \frac{1}{\mathcal{Q}H_{\rm nH}\mathcal{Q}-E_l}V_l^\dagger \\ &= -\left(J-\frac{\Omega_{\rm eff}^2}{4}\sin^2\frac{\phi}{2}\frac{1}{\delta-2J+i\kappa/2}\right)|0_A,+\rangle\langle 0_A,+| + \left(J+\frac{\Omega_{\rm eff}^2}{4}\sin^2\frac{\phi}{2}\frac{1}{\delta+2J+i\kappa/2}\right)|0_A,-\rangle\langle 0_A,-|, \\ \hat{L}_{+,\rm eff} &= |0_A,-\rangle\langle 1_A,-|\sum_l \frac{1}{\mathcal{Q}H_{\rm nH}\mathcal{Q}-E_l}V_l^\dagger = -\frac{\Omega_{\rm eff}}{2}\sin\frac{\phi}{2}\frac{1}{\delta-2J+i\kappa/2}|0_A,-\rangle\langle 0_A,+|, \\ \hat{L}_{-,\rm eff} &= |0_A,+\rangle\langle 1_A,+|\sum_l \frac{1}{\mathcal{Q}H_{\rm nH}\mathcal{Q}-E_l}V_l^\dagger = -\frac{\Omega_{\rm eff}}{2}\sin\frac{\phi}{2}\frac{1}{\delta+2J+i\kappa/2}|0_A,+\rangle\langle 0_A,-|. \end{aligned} \tag{18}$$

Therefore, we obtain the effective master equation of the atomic motion that reads

$$\begin{aligned} \frac{\partial}{\partial t}\rho_{\rm ext} &= -i[-J'\hat{\sigma}^z_{\rm ext},\rho_{\rm ext}] + \Gamma_+\mathcal{D}[\hat{\sigma}^+_{\rm ext}]\rho_{\rm ext} + \Gamma_-\mathcal{D}[\hat{\sigma}^-_{\rm ext}]\rho_{\rm ext}, \\ J' &= J + \frac{1}{2}\left(\frac{\Omega_{\rm eff}}{2}\sin\frac{\phi}{2}\right)^2 {\rm Re}\left[\frac{1}{\delta+2J+i\kappa/2}-\frac{1}{\delta-2J+i\kappa/2}\right], \\ \Gamma_+ &= \kappa\frac{\Omega_{\rm eff}^2}{4}\frac{\sin^2\frac{\phi}{2}}{(\delta-2J)^2+\kappa^2/4}, \quad \Gamma_- = \kappa\frac{\Omega_{\rm eff}^2}{4}\frac{\sin^2\frac{\phi}{2}}{(\delta+2J)^2+\kappa^2/4}. \end{aligned} \tag{19}$$

The correction to the tunnelling rate is due to H_A, which is a result of the optical potential. As shown in Fig. S1, we compare J' and J with the same parameters as used in Fig. 4, and find that relative correction of the tunnelling rate is in the order of 10^{-5}. Therefore, we neglect the correction and the tunnelling rate is still equal to J. However, in the long-term evolution, the optical potential will lead to a non-negligible phase shift for different conditions.

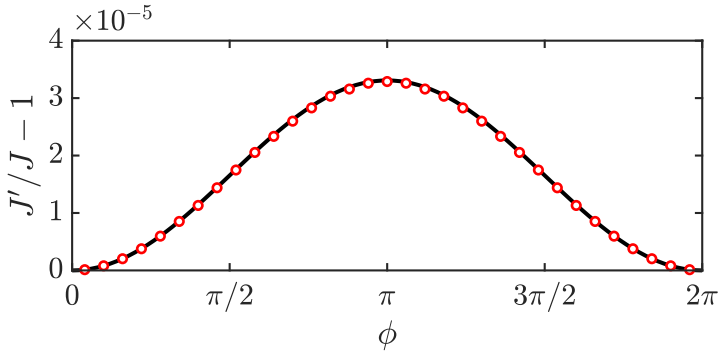

FIG. S1. The relative correction of the tunnelling rate due to the optical potential. The black line is the analytical results according to Eq. (19), the red circles are numerical results obtained from Fig. 4 (main text) with different ϕ and fitted sinusoidally in the long-time regime ($Jt > 4500$).

Then Eq. (19) gives birth to the semiclassical equation of the atomic motion ($J \approx J'$, $\Gamma = \Gamma_+ + \Gamma_-$)

$$\frac{\partial}{\partial t}\begin{pmatrix}\langle\hat{\sigma}^x\rangle\\ \langle\hat{\sigma}^y\rangle\\ \langle\hat{\sigma}^z\rangle\end{pmatrix} = \begin{pmatrix}-\Gamma/2 & -2J & \\ 2J & -\Gamma/2 & \\ & & -\Gamma\end{pmatrix}\begin{pmatrix}\langle\hat{\sigma}^x\rangle\\ \langle\hat{\sigma}^y\rangle\\ \langle\hat{\sigma}^z\rangle\end{pmatrix} + \begin{pmatrix}0\\0\\ \Gamma_- - \Gamma_+\end{pmatrix}, \tag{20}$$

Let the initial state be $|L\rangle$, $\langle\hat{\sigma}^x(0)\rangle = 1$, $\langle\hat{\sigma}^y(0)\rangle = \langle\hat{\sigma}^z(0)\rangle = 0$, the solution reads

$$\begin{aligned} \langle\hat{\sigma}^x(t)\rangle &= e^{-\frac{\Gamma}{2}t}\cos 2Jt, \\ \langle\hat{\sigma}^y(t)\rangle &= e^{-\frac{\Gamma}{2}t}\sin 2Jt, \\ \langle\hat{\sigma}^z(t)\rangle &= \frac{\Gamma_- - \Gamma_+}{\Gamma}\left(1-e^{-\Gamma t}\right). \end{aligned} \tag{21}$$

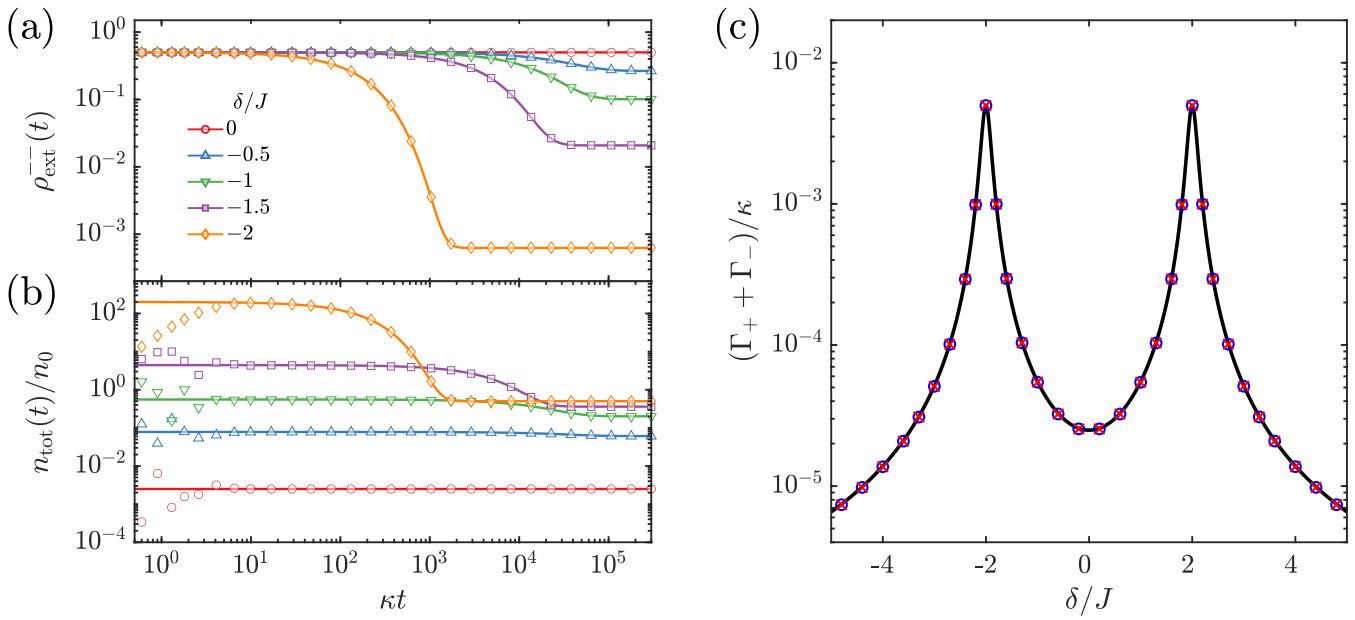

FIG. S2. Evolution of (a) the atomic population on $|-\rangle = (|L\rangle - |R\rangle)/\sqrt{2}$ state and (b) the total cavity photon numbers, $n_{\rm tot}(t)$. The double-well spacing $\phi = \pi/4$ ($d = \lambda/2$), and the initial state is $|0, 0, L, g\rangle$. The scatters are numerical simulations based on the master equation for different δ, and the dashed lines are analytical solutions according to Eq. (16). (c) The total relaxation rate, $\Gamma = \Gamma_+ + \Gamma_-$, in the long-time regime. The black line is the analytical solution, Eq. (19), and the points are exponential fitting results of the numerical simulations of (×) atomic motion, $\rho_{\rm ext}(t)$, and (∘) photon numbers, $n_{\rm tot}(t)$, respectively.

Substituting Eq. (21) to Eq. (16), one obtains the analytical solutions of the instantaneous photon numbers. For steady state, $\langle\hat{\sigma}^x(\infty)\rangle = \langle\hat{\sigma}^y(\infty)\rangle = 0$, and

$$\begin{aligned}\langle\hat{\sigma}^z(\infty)\rangle &= \frac{\Gamma_- - \Gamma_+}{\Gamma} = \frac{-4\delta J}{\delta^2 + 4J^2 + \kappa^2/4},\\ n_{\rm tot} &= n_0\left(\cos^2\frac{\phi}{2} + \frac{1}{1 + 4J^2/(\delta^2+\kappa^2/4)}\sin^2\frac{\phi}{2}\right).\end{aligned} \tag{22}$$

In Fig. S2(a,b), we present a comparison between the analytical solutions (solid lines) and numerical simulations (points). The double-well spacing for the simulation is $\phi = \pi/4$ ($d = \lambda/2$), the atom is initially in the $|L\rangle$ state, and the cavity is set to vacuum. We evaluate the saturation dynamics of the atomic tunnelling using $\rho_{\rm ext}^{--}(t)$ and compare it with Eq. (21). Similarly, we compare the photon numbers, $n_{\rm tot}(t)$, with the adiabatic solution given in Eq. (16). The numerical and analytical solutions initially do not match during the short-time dynamics of the internal states when $\kappa t < 10$. However, after $\kappa t > 10$, the analytical solutions can accurately describe the numerical simulations. We observe that for $\delta < -2J$, as J increases, the relaxation of the atomic motion slows down. Moreover, the photon numbers experience longer quasistatic plateaux before equilibrium.

In Fig. S2(c), we have fitted $\rho_{\rm ext}(t)$ and $n_{\rm tot}(t)$ with an exponential function to obtain their relaxation rates compared to Eq. (21). We observe that the numerical results agree well with the analytical solution, and the relaxation rates of the cavity photons and atomic motion are similar, implying that the relaxation of the photons keeps pace with the atomic motion. When $\delta = \pm 2J$, Γ attains the maximum value of $(g\Omega/\Delta)^2/(2\kappa)\sin^2\frac{\phi}{2}$ due to the resonant coupling between $|0_A, \pm\rangle$ and $|1_A, \mp\rangle$ states. This process leads to rapid relaxation, similar to the sideband cooling mechanism observed in optomechanics and ion traps. If $\delta \neq \pm 2J$, we expect the atom to tunnel in the double well without significant decoherence, and the light fields to adiabatically follow the atomic motion with oscillatory chirality.

III. Photon correlation of the steady state

As discussed in the main text, one can separate the Hilbert space into two subspaces based on their parity. For the steady state, the density matrix can be written as (under the basis of $|n_S, n_A, m\rangle$)

$$\begin{aligned}
&\rho_{ss} = P_+|\psi_+\rangle\langle\psi_+| + P_-|\psi_-\rangle\langle\psi_-|,\\
&|\psi_+\rangle \approx c_{00+}|00+\rangle + c_{10+}|10+\rangle + c_{01-}|01-\rangle + c_{20+}|20+\rangle + c_{11-}|11-\rangle + c_{02+}|02+\rangle,\\
&|\psi_-\rangle \approx c_{00-}|00-\rangle + c_{10-}|10-\rangle + c_{01+}|01+\rangle + c_{20-}|20-\rangle + c_{11+}|11+\rangle + c_{02-}|02-\rangle.
\end{aligned} \tag{23}$$

In the dispersive regime, the previous calculation shows that the coefficients are approximately

$$P_\pm = \frac{1}{2}\left(1 \mp \frac{4\delta J}{\delta^2 + 4J^2 + \kappa^2/4}\right) \qquad c_{00+} = c_{00-} \approx 1 \qquad c_{10+} = c_{10-} \approx \frac{\Omega_{\text{eff}}}{2}\frac{\cos\frac{\phi}{2}}{\delta + i\kappa/2}$$

$$c_{01-} \approx \frac{\Omega_{\text{eff}}}{2}\frac{\sin\frac{\phi}{2}}{\delta - 2J + i\kappa/2} \qquad c_{01+} \approx \frac{\Omega_{\text{eff}}}{2}\frac{\sin\frac{\phi}{2}}{\delta + 2J + i\kappa/2} \qquad c_{11-} \approx c_{10+}c_{01-} \qquad c_{11+} \approx c_{10-}c_{01+}$$

$$c_{20+} = c_{20-} \approx \sqrt{2}\frac{\Omega_{\text{eff}}}{2}\frac{\cos\frac{\phi}{2}}{2\delta + i\kappa}c_{10+} \qquad c_{02+} \approx \sqrt{2}\frac{\Omega_{\text{eff}}}{2}\frac{\sin\frac{\phi}{2}}{2\delta + i\kappa}c_{01-} \qquad c_{02-} \approx \sqrt{2}\frac{\Omega_{\text{eff}}}{2}\frac{\sin\frac{\phi}{2}}{2\delta + i\kappa}c_{01+}$$

For the photon mode $\hat{a}$, specifically, $\hat{a}_{\text{CW}} = (\hat{a}_S + i\hat{a}_A)/\sqrt{2}$ and $\hat{a}_{\text{CCW}} = (\hat{a}_S - i\hat{a}_A)/\sqrt{2}$, the second-order correlation is

$$g^{(2)}(\tau) = \frac{\text{Tr}\left[\hat{a}U(\tau)\hat{a}\rho_{ss}\hat{a}^\dagger U^\dagger(\tau)\hat{a}^\dagger\right]}{\text{Tr}\left[\hat{a}^\dagger\hat{a}\rho_{ss}\right]^2}. \tag{24}$$

The evolution propagator represented in the manifold consisting zero- and single-excitation states reads

$$\begin{aligned}
U(\tau) \approx\ & e^{iJ\tau}\left[|00+\rangle\langle 00+| + e^{-i\delta\tau-\kappa\tau/2}\left(|10+\rangle\langle 10+| + |01+\rangle\langle 01+|\right)\right]\\
&+ e^{-iJ\tau}\left[|00-\rangle\langle 00-| + e^{-i\delta\tau-\kappa\tau/2}\left(|10-\rangle\langle 10-| + |01-\rangle\langle 01-|\right)\right]\\
&- \frac{\Omega_{\text{eff}}}{2}\cos\frac{\phi}{2}\left[\frac{e^{-i\delta\tau-\kappa\tau/2}-1}{\delta + i\kappa/2}e^{iJt}|10+\rangle\langle 00+| + \frac{e^{-i\delta\tau-\kappa\tau/2}-1}{\delta + i\kappa/2}e^{-iJ\tau}|10-\rangle\langle 00-| + \text{H.c.}\right]\\
&- \frac{\Omega_{\text{eff}}}{2}\sin\frac{\phi}{2}\left[\frac{e^{-i(\delta+2J)\tau-\kappa\tau/2}-1}{\delta - 2J + i\kappa/2}e^{iJ\tau}|01-\rangle\langle 00+| + \frac{e^{-i(\delta-2J)\tau-\kappa\tau/2}-1}{\delta + 2J + i\kappa/2}e^{-iJ\tau}|01+\rangle\langle 00-| + \text{H.c.}\right].
\end{aligned} \tag{25}$$

The correlations of the CW and CCW modes are the same, which yields

$$\begin{aligned}
g^{(2)}(\tau) = &\left(1 + \frac{4J^2}{\delta^2 + \kappa^2/4}\right)\left[1 + \left(1 + \frac{4J^2}{\delta^2 + \kappa^2/4}\right)\cot^2\frac{\phi}{2}\right]^{-2}\left(\frac{1}{2}\left|\frac{(\delta + i\kappa/2)e^{-2iJ\tau} - 2Je^{-i\delta\tau-\kappa\tau/2}}{\delta + 2J + i\kappa/2} - \frac{\delta - 2J + i\kappa/2}{\delta + i\kappa/2}\cot^2\frac{\phi}{2}\right|^2 +\right.\\
&\left.\frac{1}{2}\left|\frac{(\delta + i\kappa/2)e^{2iJ\tau} + 2Je^{-i\delta\tau-\kappa\tau/2}}{\delta - 2J + i\kappa/2} - \frac{\delta + 2J + i\kappa/2}{\delta + i\kappa/2}\cot^2\frac{\phi}{2}\right|^2 + 4\cot^2\frac{\phi}{2}\cos^2 J\tau\right).
\end{aligned} \tag{26}$$

For a simple case, let $\delta = 0$, then the correlation function reads

$$g^{(2)}(\tau) = 1 + \left[1 + \left(1 + \frac{4J^2}{\kappa^2/4}\right)\cot^2\frac{\phi}{2}\right]^{-2}\left(\frac{4J^2}{\kappa^2/4}e^{-\kappa\tau} + \frac{4J}{\kappa/2}e^{-\kappa\tau/2}\sin 2J\tau\right). \tag{27}$$

[1] F. Reiter and A. S. Sørensen, Effective operator formalism for open quantum systems, Phys. Rev. A **85**, 032111 (2012).